


Free-Breathing Fetal Cardiac MRI With Doppler Ultrasound Gating, Compressed Sensing, and Motion Compensation

Kostas Haris, PhD,^{1,2} Erik Hedström, MD, PhD,^{2,3} Fabian Kording, PhD,⁴
 Sebastian Bidhult, PhD,^{2,5} Katarina Steding-Ehrenborg, MD, PhD,^{2,6} Christian Ruprecht, PhD,⁴
 Einar Heiberg, PhD,^{2,5} Håkan Arheden, MD, PhD,² and Anthony H. Aletras, PhD^{1,2*} 

Background: Fetal cardiovascular MRI complements ultrasound to assess fetal cardiovascular pathophysiology.

Purpose: To develop a free-breathing method for retrospective fetal cine MRI using Doppler ultrasound (DUS) cardiac gating and tiny golden angle radial sampling (tyGRASP) for accelerated acquisition capable of detecting fetal movements for motion compensation.

Study Type: Feasibility study.

Subjects: Nine volunteers (gestational week 34–40). Short-axis and four-chamber views were acquired during maternal free-breathing and breath-hold.

Field Strength/Sequence: 1.5T cine balanced steady-state free precession.

Assessment: A self-gated reconstruction method was improved for clinical application by using 1) retrospective DUS gating, and 2) motion detection and rejection/correction algorithms for compensating for fetal motion. The free-breathing reconstructions were qualitatively and quantitatively assessed, and DUS-gating was compared with self-gating in breath-hold reconstructions. A scoring of 1–4 for overall image quality, cardiac, and extracardiac diagnostic quality was used.

Statistical Tests: Friedman's test was used to assess differences in qualitative scoring between observers. A Wilcoxon matched-pairs signed rank test was used to assess differences between breath-hold and free-breathing acquisitions and between observers' quantitative measurements.

Results: In all cases, 111 free-breathing and 145 breath-hold acquisitions, the automatically calculated DUS-based cardiac gating signal provided reconstructions of diagnostic quality (median score 4, range 1–4). Free-breathing did not affect the DUS-based cardiac gated retrospective radial reconstruction with respect to image or diagnostic quality (all $P > 0.06$). Motion detection with rejection/correction in k -space produced high-quality free-breathing DUS-based reconstructions [median 3, range (2–4)], whereas free-breathing self-gated methods failed in 80 out of 88 cases to produce a stable gating signal.

Data Conclusion: Free-breathing fetal cine cardiac MRI based on DUS gating and tyGRASP with motion compensation yields diagnostic images. This simplifies acquisition for the pregnant woman and thus could help increase fetal cardiac MRI acceptance in the clinic.

Level of Evidence: 2

Technical Efficacy Stage: 1

J. MAGN. RESON. IMAGING 2020;51:260–272.

View this article online at wileyonlinelibrary.com. DOI: 10.1002/jmri.26842

Received Mar 4, 2019, Accepted for publication Jun 4, 2019.

*Address reprint requests to: A.H.A., Laboratory of Computing, Medical Informatics and Biomedical-Imaging Technologies, Aristotle University of Thessaloniki, School of Medicine, Box 323, Thessaloniki, GR-54124, Greece. E-mail: aletras@hotmail.com

Contract grant sponsors: Swedish Heart and Lung Foundation, Swedish Research Council, the Medical Faculty at Lund University, Skåne University Hospital, Lund, and Region of Skåne.

From the ¹Laboratory of Computing, Medical Informatics and Biomedical-Imaging Technologies, School of Medicine, Aristotle University of Thessaloniki, Thessaloniki, Greece; ²Department of Clinical Sciences Lund, Clinical Physiology, Lund University, Skåne University Hospital, Lund, Sweden; ³Department of Clinical Sciences Lund, Diagnostic Radiology, Lund University, Skåne University Hospital, Lund, Sweden; ⁴Department of Diagnostic and Interventional Radiology, University Medical Center Hamburg-Eppendorf, Hamburg, Germany; ⁵Department of Biomedical Engineering, Faculty of Engineering, Lund University, Lund, Sweden; and ⁶Department of Health Sciences, Physiotherapy, Lund University, Lund, Sweden

This is an open access article under the terms of the Creative Commons Attribution-NonCommercial License, which permits use, distribution and reproduction in any medium, provided the original work is properly cited and is not used for commercial purposes.

FETAL CARDIAC magnetic resonance imaging (MRI) is being increasingly used complementary to ultrasound for the assessment of the developing fetus.¹ High spatiotemporal resolution MR images of the fetal heart can be useful clinically in challenging cases of cardiovascular malformation where ultrasound and anatomical imaging alone are insufficient.²⁻⁴

The challenges of developing fetal cardiac MRI are well documented.⁵⁻¹⁰ Some of these include: 1) fetal heart anatomy: small size within a large field of view (FOV) with distance to coil implying low signal-to-noise ratio (SNR); 2) lack of a usable fetal ECG: acquisition and extraction of fetal ECG is not solved, making the required gating process a central issue; 3) periodic motion: high heart rate with high variability combined with maternal respiration; and 4) Stochastic fetal movements: unpredictable and spontaneous movements of the fetus result in both in- and through-plane and rotational displacement.

High fetal heart rates impose the requirement of rapid k -space data acquisition that can be accomplished by parallel imaging and compressed sensing.¹¹ Both approaches rely on accelerating the acquisition by means of k -space undersampling and are combined in a multicoil sparsity application, iterative Golden angle Radial Sparse Parallel MRI (iGRASP).¹²⁻¹⁷ An improved version of iGRASP, free of the eddy current problems caused by the large golden angle increment, referred to as tyGRASP, is based on the tiny (ty) golden angles introduced by Wundrak et al.¹⁸

Breath-holding during image acquisition is sufficient to eliminate respiratory movements but can be challenging for the pregnant woman. Breath-hold acquisitions should thus be either avoided by applying free-breathing techniques or short acquisition times (preferably below 12 sec).

The lack of a fetal ECG can be handled by retrospective self-gated techniques that estimate the synchronization signal by processing the acquired k -space data.¹⁹ However, these methods may require user interaction, since the periodic motion of the small fetal heart is very weakly projected to the center of the k -space spokes in the case of radial sampling. Metric optimized gating (MOG) is a semiautomated and computationally demanding method; however, yielding high-resolution images.^{10,20,21} A promising approach towards accurate retrospective cardiac gating is the Doppler ultrasound (DUS) method,^{22,23} as magneto-hydro-dynamic effects do not influence the method.

Stochastic fetal movement is a more challenging problem.²¹ Whereas in-plane movement does not alter the imaged anatomy and compensation in k -space is possible through image registration algorithms,^{21,22} through-plane movement cannot be adjusted this way. A promising integrated approach towards this direction was recently proposed by Roy et al.²¹ However, the required real-time reconstruction for motion detection and compensation imposes a tremendous computational load, presumes an accurate cardiac gating signal, and automated artifact-free compressed sensing reconstruction from severely undersampled radial k -space data. Another recent free-breathing reconstruction approach proposed by van Amerom et al.²⁴ is based on retrospective processing of

highly accelerated dynamic MRI. Parallel imaging and compressed sensing are utilized by the initially applied Cartesian k - t SENSE reconstruction method,²⁵ which is semiautomatic, as it depends on a user-defined fetal cardiac region of interest (ROI). These high-quality results, however, show a promising image-domain fetal cardiac MRI application.

In this work, we propose a novel integrated free-breathing/short breath-hold fetal cardiac MRI reconstruction method combining DUS-based gating and compressed sampling with parallel imaging through the tyGRASP framework to speed up and automate the reconstruction process. We hypothesized that quantitative and qualitative evaluations by experienced observers of fetal cine cardiac MR images for breath-held and free-breathing acquisitions would be comparable.

Materials and Methods

Reconstruction Method

OVERVIEW. The proposed reconstruction method stages are shown in Fig. 1. First, the reconstruction speed was increased by reducing the number of receiver coil channels using a channel compression algorithm. Next, the cardiac gating (CG) signal was extracted by analyzing the DUS input signals. The CG signal provided the RR intervals (DUS triggers) that were input to the subsequent stages: 1) motion detection and correction/rejection and 2) retrospective cardiac gating. Finally, the resulting re-sorted radial projections were used to reconstruct fetal cardiac cine images via the tyGRASP method. A more detailed presentation of these stages follows below.

DATA ACQUISITION. Fetal cardiac MRI data were acquired using the tiny golden angle radial trajectory scheme of order 7. This radial sampling scheme is a generalization of the golden-angle radial scheme.^{17,26} Tiny golden angles act as golden angle surrogates, retain most of the properties of the golden angle sampling scheme, ie, approximately uniform coverage of k -space and sampling incoherence, and cause remarkably weaker eddy current artifacts.^{18,27}

MRI COIL COMPRESSION. The extreme computational requirements caused by the large coil arrays (up to 60 coils), used for parallel imaging, were drastically reduced with linear dimensionality reduction methods. Specifically, we applied the coil compression approach proposed by Huang et al.,²⁸ modified so that all available k -space data were input to the principal component analysis module.

DUS SIGNAL PROCESSING FOR GATING SIGNAL EXTRACTION

The signal peaks output from the DUS (North Medical, Hamburg, Germany)²³ were used for cardiac gating (Fig. 2). The DUS device assessed fetal cardiac blood flow and neglected the effect of myocardial wall motion through high-pass filtering. The resulting DUS signal was input to a peak detection module where peaks were located using adaptive thresholding,

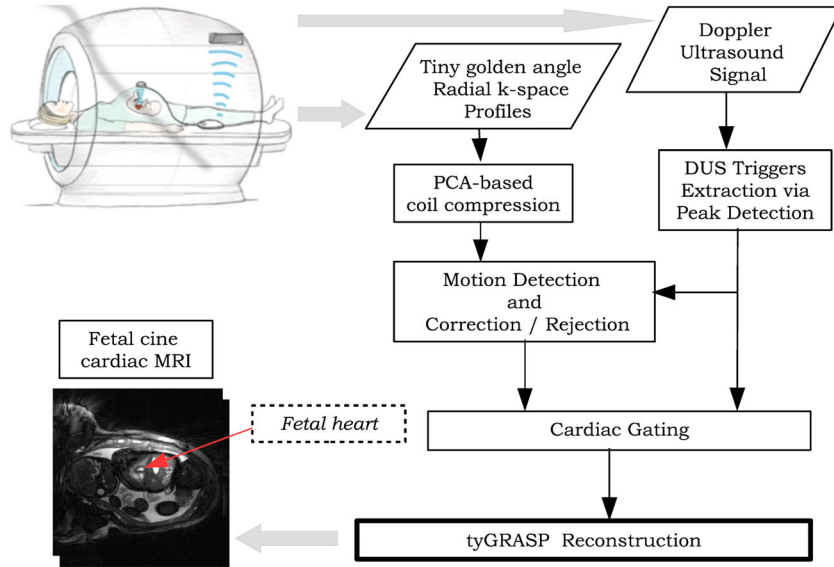


FIGURE 1: Flowchart of the DUS-gated fetal cardiac reconstruction method.

autocorrelation analysis, and wavelet transforms.²⁹ The detected DUS peaks represented the cardiac cycles (RR intervals) and were used for sorting the radial k -space profiles into the cardiac phases.¹³ The absence of DUS triggers during acquisition was considered an indicator of considerable fetal movement and was used for excluding the corresponding radial profiles for reconstruction. However, successful detection of DUS triggers did not necessarily indicate a quiescent period, as the DUS signal detection is not sensitive to shallow fetal movement or maternal breathing.

MOTION DETECTION AND DATA REJECTION/CORRECTION. Motion detection and subsequent correction or rejection of k -space data were accomplished in two stages: 1) a low-temporal resolution reconstruction (described in more detail below) was performed to allow for visual inspection and manual identification of acquisition periods containing either major fetal movement, rejected before further analysis, or no fetal movement or minor respiratory and/or in-plane translational movements of the fetus, referred to as quiescent/semiquiescent periods. A real-time reconstruction could serve this purpose²¹ but it is computationally demanding both in time and memory. The k -space data of the quiescent/semiquiescent periods were input to the stage of motion estimation and correction (Fig. 3) which was based on the following low temporal resolution reconstruction (LTR)³⁰: for each

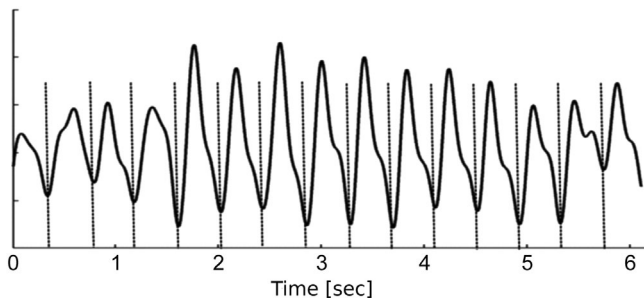


FIGURE 2: DUS signal trace and corresponding trigger signal.

cardiac cycle, only one image was reconstructed using the corresponding radial profiles. The motion of the pulsating fetal heart was smoothed out and displacements depicted in these images were due to maternal respiration and/or translational fetal movements, as the visual inspection process had rejected data containing other types of movement. Movements were estimated via translational registration (Fig. 3): the first of the N reconstructed images were taken as reference (fixed) and, for each of the remaining $N-1$, the best shift S_x, S_y was computed as the solution of a sum-of-squares minimization problem. Thereafter, corresponding k -space radial profiles were appropriately shifted by interpolation.²¹ Registration was applied for an ROI including the fetal heart as movements within this region were to be corrected.

TYGRASP RECONSTRUCTION. Under the tyGRASP formulation introduced by Wundrak et al²⁷ as an improvement of iGRASP,¹² the reconstruction problem was reduced to the minimization:

$$\hat{\mathbf{d}} = \min_{\mathbf{d}} \left\{ \underbrace{\|\mathbf{F} \cdot \mathbf{S} \cdot \mathbf{d} - \mathbf{m}\|_2^2}_{\text{multi-coil data fidelity}} + \lambda \underbrace{\|\nabla_t \mathbf{d}\|_1}_{\text{temporal sparsity}} + \mu \underbrace{\|\nabla_s \mathbf{d}\|_1}_{\text{spatial sparsity}} \right\}, \quad (1)$$

where \mathbf{d} was the fetal cardiac image sequence to be reconstructed in x - y - t space; ∇_t, ∇_s were the temporal and spatial total-variation operators; $\mathbf{m} = [m_1, m_2, \dots, m_c]$ were the acquired multicoil radial k -space data with c coils; \mathbf{F} was the multicoil NUFFT gridding operator³¹ defined on the radial acquisition pattern; $\mathbf{S} = [S_1, S_2, \dots, S_c]$ were the coil sensitivity maps for c coils; and λ and μ were the

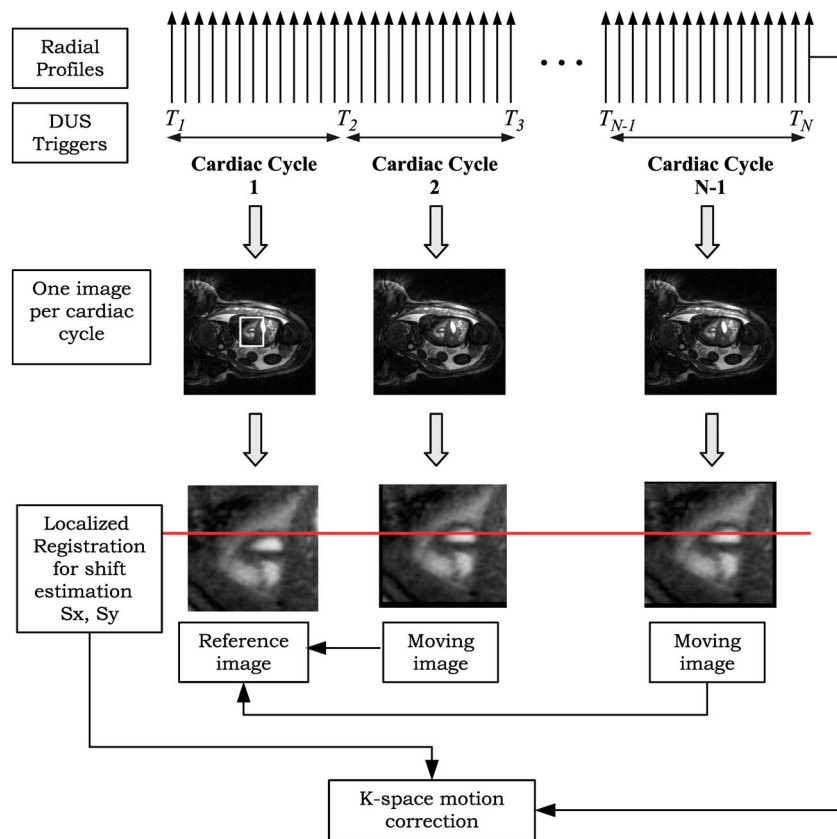


FIGURE 3: Translational motion estimation and correction in k -space.

temporal and spatial regularization parameters. Typical λ, μ values were in the range of 0.01 to 0.1 and 0.0005 to 0.001, respectively. The optimization problem in Eq. [1] was solved by the nonlinear conjugate gradient with backtracking line search.³²

The algorithms were implemented in MatLab (2015a, MathWorks, Natick, MA). All reconstructions were performed offline on a personal computer.

Fetal Cardiac Image Acquisition

The regional Ethics Review Board approved the study and written informed consent was obtained before participation ($n = 9$ pregnant women; 27–43 years; gestational week 34–40). Exams were performed on a 1.5T Magnetom Aera scanner (Siemens Healthcare, Erlangen, Germany). A prototype MRI-compatible DUS device was used to acquire the movement of blood through the fetal heart during cine image acquisition. These data were input for gating the acquired tyGRASP images to the fetal heart-beat during the offline reconstruction. The research subject was placed in the left decubitus position and all acquisitions were performed within a maximum limit for specific absorption rate of 2 W/kg. The DUS transducer was placed over the fetal chest as located by palpation and fastened using an elastic belt. Signal quality and triggering were checked for consistency during 30 seconds before entering the bore. Data were acquired using a combination of a phased body-array 18-channel coil and a phased spine-array 32-channel coil. The fetal heart short-axis and four-chamber views were located using an interactive scan-plan sequence, limited in flip angle, spatial resolution, and time applied to avoid unnecessary energy deposition. Thereafter, the radial tyGRASP cine acquisitions with tiny golden angles of order 7 (μ_7) were acquired. As this setup resulted in no visible eddy current

artifacts, no further eddy current calibration or correction was performed. Typical sequence parameters were: echo time / repetition time (TE/TR) = 1.88/3.7 msec, flip angle 60° , pixel size $0.7 \times 0.7 \times 4 \text{ mm}^3$, matrix size 256×256 . For each volunteer, stacks covering the ventricles including a total of 13 short-axis and five four-chamber slices were acquired. Acquisitions were performed during maternal free-breathing with 4000 radial spokes per slice, and during breath-hold applying 3000 radial spokes per slice, resulting in 162 sets of 4000 free-breathing profiles and 162 sets of 3000 breath-hold profiles (each set corresponding to a slice). From these sets, 51 breath-hold and 17 free-breathing sets were rejected due to DUS-device signal loss or major continuous fetal movement (Table 1).

All volunteers completed the MRI scan protocol and were included for analysis. The total scan time for complete cine sets including sequence preparation times, localizer planes, and repeated localizer acquisition when needed was ~ 5 minutes per volunteer. Typical reconstruction times with the proposed method described in Fig. 1 were ~ 15 minutes per slice with MatLab on a medium performance computer. In cases where there was fetal movement (57/145 for free-breathing and 62/111 for breath-hold), the observer visually selected the longest quiescent/semiquiescent acquisition period to be used for the proposed retrospective reconstruction. A quiescent/semiquiescent acquisition period was a sequence of consecutive radial profiles containing no major fetal movement or major in-plane translational movement due to free-breathing or shallow fetal movement. In these cases, reconstruction time was increased to 20 minutes per slice. As described earlier, quiescent/semiquiescent acquisition periods were visually detected by the examination of the low temporal resolution image reconstruction and corrected in k -space by the estimated registration-based translation.

TABLE 1. Available Datasets (Acquisitions) for Image Reconstruction of the Nine Fetuses

Fetus nr	1	2	3	4	5	6	7	8	9	Total
Breath-hold	4	15	18	15	13	8	9	17	12	111
Free-breathing	18	18	18	18	17	17	3	18	18	145
										256
Avg heart rate (bpm)	137	130	147	152	126	133	113	153	132	

A table cell of the breath-hold and free-breathing rows can correspond to a maximum of 18 acquisitions. The reported number in each cell represents the raw k-space datasets after discarding datasets due to DUS signal loss or severe fetal movement. For example, for the breath-hold acquisition of fetus 1 only 4 datasets out of 18 were retained. In total, 111/162 breath-hold and 145/162 free-breathing datasets were used for reconstruction (51/162, 17/162, respectively were rejected). The last row of the table shows the average heart rate during the examination of each fetus.

Motion Correction Evaluation

Successful motion correction was expected to compensate for fetal movement, thus canceling blurring effects and resulting in sharper reconstructed images. However, the original cine images were not known, and therefore the quantitative evaluation of motion correction was a challenge. We followed the approach proposed previously^{21,33,34} where the relative spatial blur between pre- and postmotion corrected

images was evaluated. In short, let I_s be a sharp image and I_b a blurred version of it. The *spatial blur* of I_b relative to I_s was defined as the value of sigma parameter, s , of the Gaussian smoothing kernel for which the normalized root-mean-squared error between the smoothed sharp image ($I_s * G(s)$) and I_b is minimized (Fig. 4).

The proposed motion correction and evaluation methods were tested in a simulated translational periodic respiration-like movement

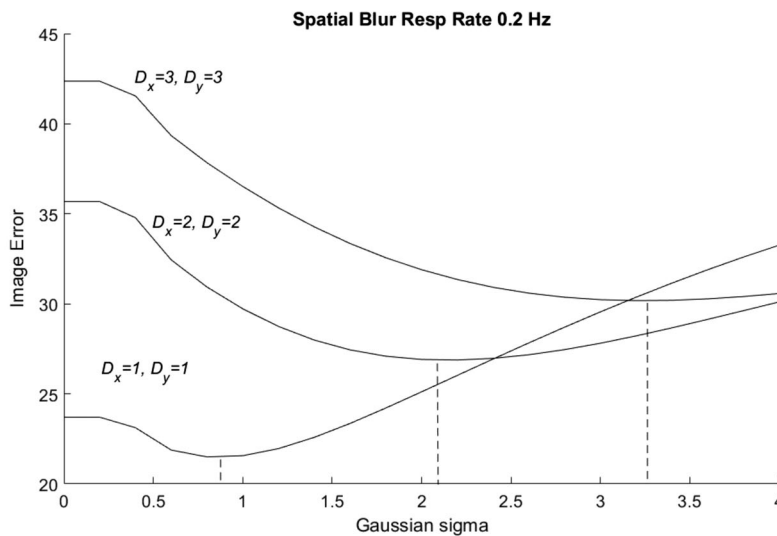
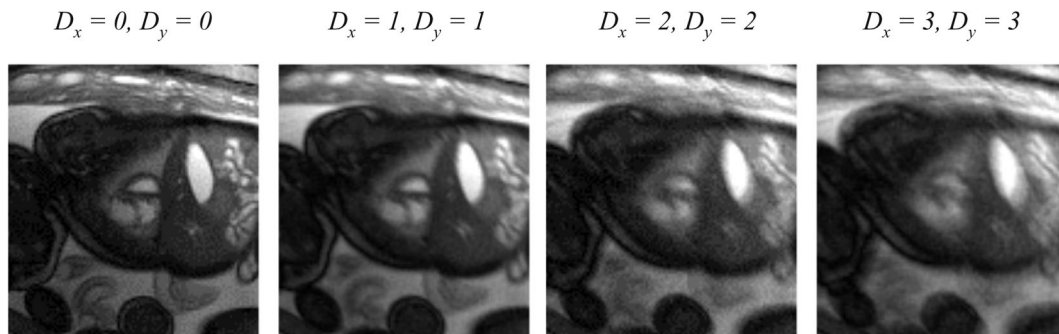


FIGURE 4: Spatial blur estimation for various translational shifts in k-space via simulated respiration. Top row, left to right: The initial motion-free reconstruction and the corresponding reconstructions of uncorrected k-space data containing simulated translational motion of maximum shift $D_x, D_y = 1, 2, 3$ pixels, respectively. The motion-induced blurring effect is evident. Bottom row: The value of Gaussian sigma that corresponds to the local minimum (dotted vertical lines) of the error of the Gaussian smoothed initial image and the corresponding blurred image.

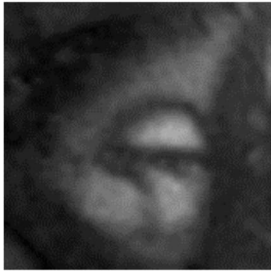

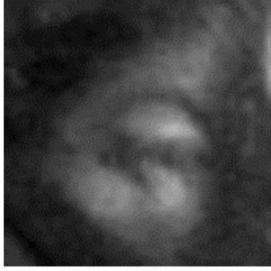

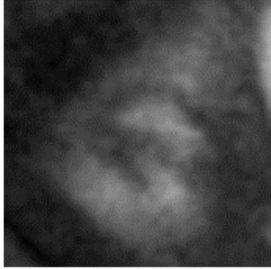

Shift D_x, D_y	Reconstruction without Motion Correction	Reconstruction with Motion Correction
1		
2		
3		

FIGURE 5: Indicative end-diastolic frames of reconstructions without and with motion correction for simulated translational respiration with maximum shift 1, 2, and 3 pixels, respectively.

setting as follows: A breath-hold fetal dataset carefully selected to be free from fetal movement was reconstructed. The absence of motion of any type resulted in high-quality reconstructions with sharp borders. Then a periodic translational motion was simulated by shifting the k -space data according to the equations: $S_x(t) = D_x \sin(2\pi f t)$,

$S_y(t) = D_y \sin(2\pi f t)$, where f is the respiration frequency taking values in the range $[0.2, 0.3]$, and D_x, D_y are the maximum horizontal and vertical displacements in pixels, respectively. Next, the motion detection algorithm was applied and its ability to estimate the simulated spatial shifts was assessed. Then shifted data were reconstructed with and without motion correction (Fig. 5).

Fetal Cardiac Image analysis

Image evaluation was performed in Segment v2.0.³⁵ Three observers (H.A., E.H., K.S.E. with 25, 19, and 14 years of experience, respectively) determined overall image quality, cardiac and extracardiac diagnostic quality. Two observers (E.H. and K.S.E.) measured septal wall thickness, and right and left lumen diameter between septum and the corresponding lateral wall at end-diastole and end-systole (Fig. 6)

Qualitative assessment was based on 4-graded scales. For overall image quality: 1 = low quality and/or high degree of artifacts; 2 = moderate quality and/or some artifacts; 3 = high quality and/or few artifacts; and 4 = high quality and no artifacts. For cardiac diagnostic quality: 1 = inadequate; 2 = low; 3 = moderate; and 4 = high. The basis for diagnostic quality included discernible epi- and endocardial borders to surrounding tissue and blood pool, visualized papillary muscles/trabeculation, visualized wall thickening during contraction, and potential of measurement of wall thickness and diagnosis of cardiac pathology. For extracardiac diagnostic quality: 1 = inadequate; 2 = low; 3 = moderate; and 4 = high, based on thoracic structures outside the heart, brain structures, contrast between brain and cerebrospinal fluid, spinal cord visualization, abdominal structures, and placental structure and attachment.

Statistical analysis

Statistical analyses were performed using GraphPad (Prism v. 8.0.2, La Jolla, CA). Data are presented as median (range) or median [interquartile range]. Friedman’s test was used to assess differences in qualitative scoring between observers. The Wilcoxon matched-pairs signed rank test was used to assess differences between breath-hold and free-breathing acquisitions and between observers’ quantitative measurements. Paired Student’s t -test was used to discern statistically

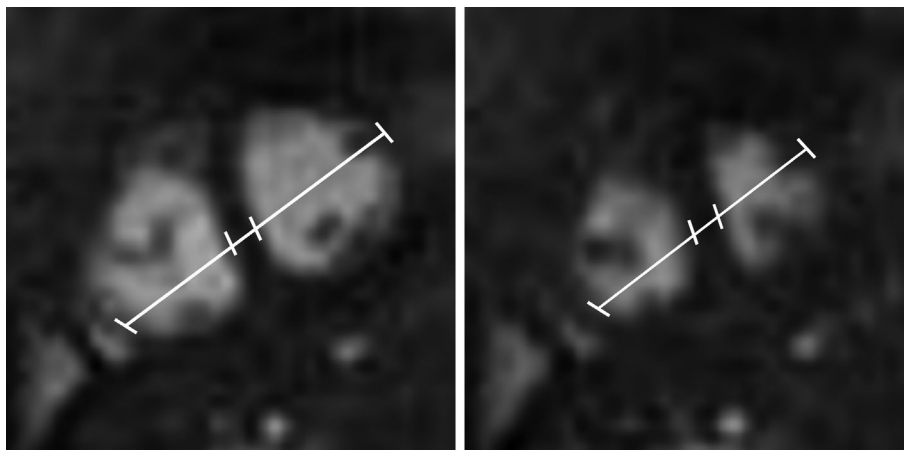


FIGURE 6: Measurements of septal wall thickness, right and left ventricular lumen widths. Measurements were performed on a midventricular level along the 4-chamber plane as indicated by the white solid line with dividers for the septum and endmarkers at the endocardium of the right and left ventricle, at end-diastole (left) and end-systole (right).

TABLE 2. DUS-Based Visual Scoring of Overall Image Quality, Cardiac and Extracardiac Diagnostic Quality by Three Experienced Observers

Case #	Observer 1			Observer 2			Observer 3		
	Overall quality	Cardiac diagnostic quality	Extracardiac diagnostic quality	Overall quality	Cardiac diagnostic quality	Extracardiac diagnostic quality	Overall quality	Cardiac diagnostic quality	Extracardiac diagnostic quality
1	4	4	4	4	4	4	4	4	3
2	3	3	3	4	3	4	3	3	4
3	4	4	4	4	4	4	4	4	4
4	4	4	4	4	3	4	4	4	4
5	4	4	4	3	4	3	4	4	3
6	3	3	4	3	2	3	4	2	2
7	4	4	4	4	4	4	3	4	3
8	3	4	4	3	4	3	4	3	4
9	4	3	4	4	3	4	3	4	4
Median (range)	4 (3-4)	4 (3-4)	4 (3-4)	4 (3-4)	4 (2-4)	4 (3-4)	4 (3-4)	4 (2-4)	4 (2-4)
Free-breathing acquisition	Overall quality	Cardiac diagnostic quality	Extracardiac diagnostic quality	Overall quality	Cardiac diagnostic quality	Extracardiac diagnostic quality	Overall quality	Cardiac diagnostic quality	Extracardiac diagnostic quality
1	3	4	4	3	4	3	3	3	3
2	3	4	4	4	4	4	3	4	4
3	3	4	2	2	3	2	3	4	2
4	4	3	4	4	4	4	4	3	3
5	3	4	4	3	4	3	3	4	3
6	3	3	3	3	3	3	3	3	2
7	3	4	3	2	4	2	3	4	3
8	4	4	4	3	4	3	4	4	4
9	2	3	3	2	3	2	2	4	3
Median (range)	3 (2-4)	4 (3-4)	4 (2-4)	3 (2-4)	4 (3-4)	3 (2-4)	3 (2-4)	4 (3-4)	3 (2-4)

All $P > 0.09$ between observers; all $P > 0.06$ between breath-hold and free-breathing acquisitions.

significant differences between heart rates by self-gating and DUS. Differences with $P < 0.05$ were considered significant.

Results

In breath-hold acquisitions containing no movement of any type (49/111), mean self-gating and DUS-gating heart rates were not found to be significantly different ($P = 0.293$). However, in all cases the self-gated approach required interactive adjustment of the fetal cardiac heart rate for bounding the frequency search window, while the DUS-gated approach is completely parameter-free and automatic. This saved ~10–15 minutes/slice in reconstruction time.

In free-breathing acquisitions containing only maternal respiratory motion (88/145 sets), the DUS-based cardiac gating was sufficiently accurate to support the cardiac gating stage without further need of manual correction. Maternal breathing introduced small to negligible translational movement of the fetal heart without downgrading image quality with regard to the beating fetal heart, compared with breath-hold acquisitions (Table 2). Extracardiac anatomical structures that had undergone relatively larger movement resulted in visually lower-quality reconstruction due to motion-induced blur; however, not significantly (Table 2; all $P > 0.18$ between breath-hold and free-breathing acquisitions). However, the self-gated reconstruction of free-breathing acquisitions failed to provide images of acceptable quality in 80 out of 88 cases (91%) because the estimated CG signal resulted in highly erroneous binning.

In acquisitions with partially missing DUS triggers (24/256, both free-breathing and breath-hold), DUS signal loss signified

major fetal movement. This was verified by visual examination of low temporal resolution image reconstruction images using interpolated triggers for periods without DUS triggers. Therefore, radial profiles corresponding to lack of triggers were rejected since those radial profiles contain mismatched anatomical information while the remaining ones were used for reconstruction.

The remaining acquisitions (62/111 breath-hold and 57/145 free-breathing cases) corresponded to cases with available DUS triggers but in which the fetus exhibited various types of movement. Identification of the type of fetal movement and duration was based on the visual examination of the low temporal resolution image reconstruction.

Figure 7 shows LTR reconstructions revealing high deformable fetal movements. In all cases rejection of the radial profiles corresponding to fetal movements resulted in improved reconstruction quality by one or two grades in the 4-graded scale used (final scores listed in Table 2). An example of reconstruction before and after rejection of the radial profiles containing movement is shown in Fig. 8. In eight cases fetal movement was identified as in-plane translational motion and Fig. 9 shows an example of a motion-correction case, which provided anecdotal evidence that registration-based motion correction in such cases may result in improved myocardial edge definition.

Overall image quality, cardiac diagnostic quality, and extracardiac diagnostic quality were similar between breath-hold and free-breathing acquisitions and between observers (Table 2; all $P > 0.09$ between observers; all $P > 0.06$ between breath-hold and free-breathing acquisitions).

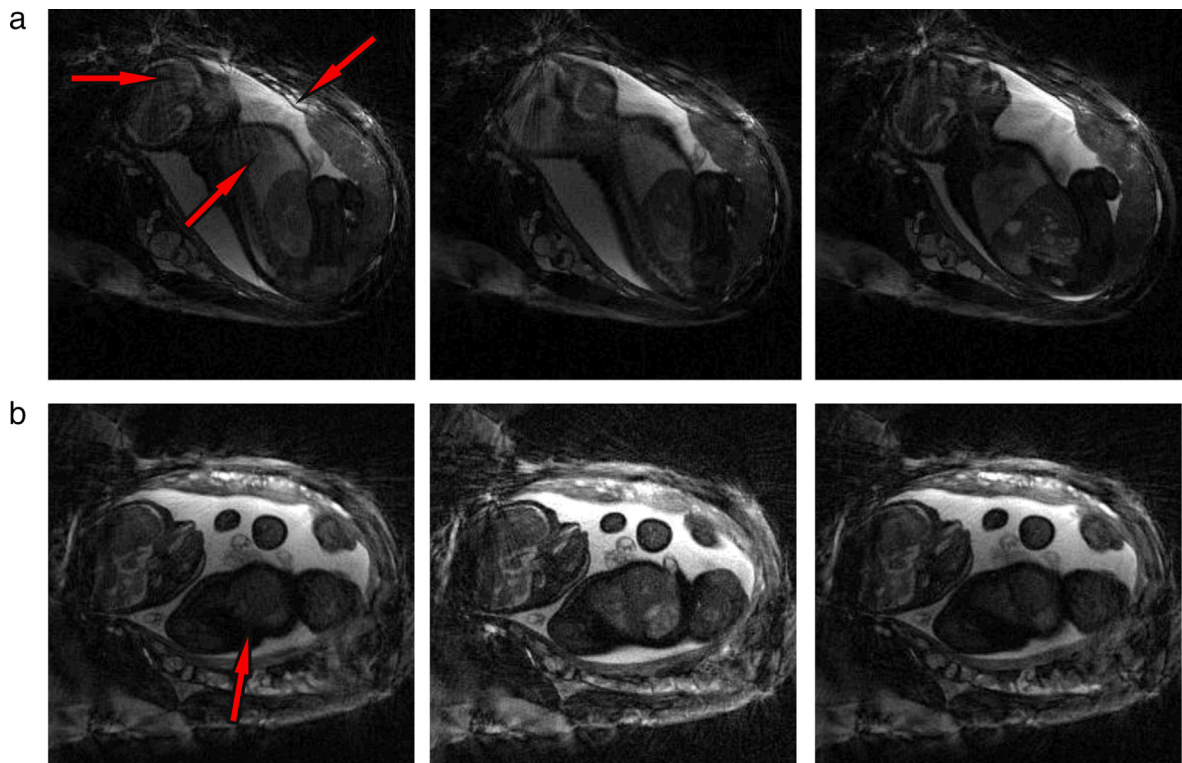


FIGURE 7: Low temporal resolution reconstruction frames with highly deformable fetal movement (a) and through-plane movement (b). Arrows in the first frame indicate areas under deformation/movement.

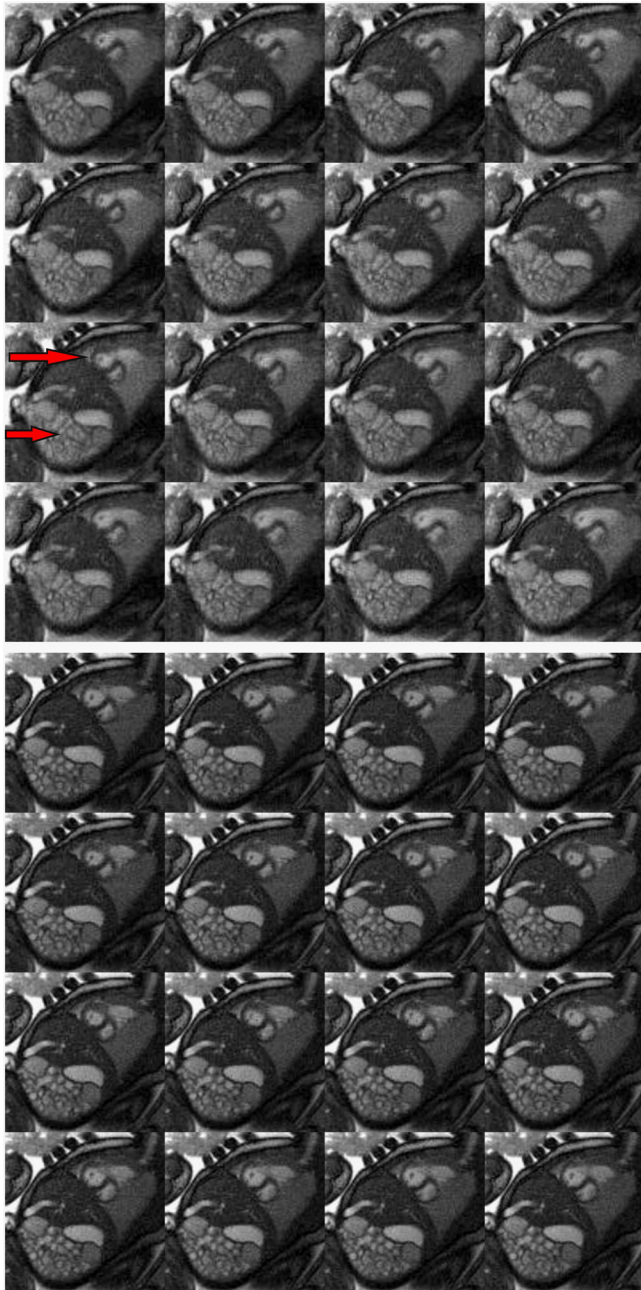


FIGURE 8: Reconstructed cardiac phases before (top) and after (bottom) rejection of radial profiles containing motion. Arrows indicate areas where blurring due to movement was reduced after rejection.

Quantitative end-diastolic and end-systolic measurements of wall thickness, right lumen diameter, and left lumen diameter showed agreement between breath-hold and free-breathing acquisitions (Table 3; all $P > 0.28$). Bias between breath-hold and free-breathing acquisitions were for wall thickness (end-diastole: 0 [0–0] mm; end-systole: 0 [0–0] mm), right lumen diameter (end-diastole: –0 [–1–0] mm; end-systole: 0 [–1–1] mm), and left lumen diameter (end-diastole: 0 [–1–0.5] mm; end-systole: 0 [–0.5–0.5] mm). Interobserver agreement was for septal thickness, right and

left lumen diameter at end-diastole in free-breathing acquisitions 0 [0–0] mm (0 [0–0] %), 0 [–1–1] mm (0 [–7–7] %) and –0.5 [–0.5–0] mm (–5 [–5–0] %), respectively. Corresponding interobserver agreement at end-systole was 0 [0–0] mm (0 [0–0] %), –1 [–1.5–0.5] mm (–9 [–11–7] %) and –0.5 [–1–0] mm (–5 [–14–0] %), respectively.

Discussion

A free-breathing DUS-gated fetal cardiac cine MRI retrospective reconstruction method combining sparse radial sampling with parallel imaging and motion correction was presented. It constitutes a major improvement of the recent method¹³ for self-gated fetal cardiac cine MRI in two ways: 1) DUS-based cardiac gating is more accurate and robust compared with self-gated reconstruction, and 2) motion detection and correction allows for free-breathing multislice acquisitions, since the examination can be well tolerated by pregnant women. Scanner calibration was avoided, since the use of the tiny golden angle radial sampling scheme drastically reduced eddy currents and subsequent artifacts.

Radial streak artifacts were the main reason for slightly degraded overall image quality in both breath-hold (median score 4) and free-breathing acquisitions (median score 3). However, in most cases it did not affect diagnostic quality (median score 4 for both breath-hold and free-breathing acquisitions). In cases where particular regions would be of interest for clinical evaluation, reacquisition of images with either the FOV rotated or moved would move the artifacts sufficiently to provide diagnostic quality.

The most crucial part of the reconstruction pipeline is the extraction of accurate gating signal, as inaccurate cardiac gating results in misclassification of the radial profiles into the wrong cardiac phases (bins), thus degrading reconstruction quality. In addition, the presence of major fetal movement that alters which part of the fetus is imaged during acquisition may make even accurate gating useless, since different projections of the fetal anatomy are mixed. Therefore, the most appropriate approach for reconstructions of acceptable quality is the application of accurate cardiac gating on either acquisition periods with no movement, or semiquiescent acquisition periods with minor movement amenable to estimation and motion correction. Towards this direction, the DUS-based cardiac gating is advantageous because major fetal movement results in DUS signal loss. Radial profiles corresponding to periods of no DUS signal were better rejected and not used in the reconstruction process, inherently improving gating quality. This improvement to the previous self-gated approach¹³ was crucial. Previously, the presence of major fetal movement either prevented the detection of accurate cardiac gating signal for the whole acquisition of radial profiles or failed to detect the quiescent/semiquiescent periods to guide radial profile rejection. This explains the necessity of breath-hold acquisitions when applying the self-gated approach and its zero tolerance to movement of any type. This was also confirmed by



FIGURE 9: Reconstructed cardiac phases without (left) and with (right) translational motion estimation and correction. After motion correction the motion-induced blur is clearly reduced (as indicated for heart and spine by red arrows).

the current study, showing failure to reconstruct free-breathing acquisitions by self-gating in 91% of the cases.

In the current center, either a technologist or a junior doctor with previously no or little experience in obstetrics placed the DUS transducer. They had received only short practical training on how to palpate the fetal position and how to place the transducer. Nevertheless, the success rate was 100% after training in 10 clinical cases. In most cases, there was a good DUS triggering/gating signal for 30 minutes. In cases where repositioning was needed, this was usually only about moving the center of the transducer ~5–10 cm. A multiarray transducer would solve this but it was not available. In instances where the DUS signal was lost, it was more often either earlier in pregnancy or in cases with a small fetus, having relatively more intrauterine space to move about. Maternal obesity or very complex fetal cardiac malformation with extrathoracic vessels increases the challenge to getting a good triggering/gating signal. Maternal breath-holding can lead to signal dropout, as supported by the current data, with more data rejected than during free-breathing acquisition. Therefore, the free-breathing acquisition as presented in the current study is an important step towards more widely available fetal cardiac MRI, with improved quality in more cases.

The identification of the quiescent/semiquiescent periods by the visual inspection of the LTR reconstruction images may raise concerns about inter- and intraobserver variability and its consequences to the reconstruction quality. However, in practice this was not an issue: First, the LTR image sequence was inherently approximate because for each fetal heart cycle only one image was reconstructed. Therefore, the temporal resolution was one heart cycle. In addition, the

nature of fetal movements, which are spontaneous and large, makes their detection easier. Finally, potential discarding of a slightly larger portion of k -space data, which may not contain fetal movement, would not downgrade the reconstruction quality.

The large variation of possible fetal movement in 3D space, frequently deformable, makes the case of purely translational in-plane movements a relatively infrequent movement type, thus reducing the applicability of that motion correction alone. However, reconstructions based on visually identified quiescent periods of short duration covering only five to six fetal heart cycles, ie, less than 3 seconds, were of adequate diagnostic quality. This implies that the method may be applied clinically for prenatal diagnosis of cardiovascular malformation close to delivery, as it provided diagnostic images by discarding data when the fetus moved and images were relatively quickly reconstructed on a medium performance computer. Nevertheless, as the method is currently on offline reconstruction, refinement and full automation is needed for making the proposed method widely available. In addition, the fact that the in-plane translational fetal movement is rare constitutes a strong indicator that the fetal heart motion correction problem should not be addressed by processing isolated 2D slices. A more promising direction is the 3D extension of the proposed motion correction method where more realistic fetal heart motion models could be used. Such models have been used for the 3D reconstruction of fetal brain and some early feasibility results for fetal heart cases have been published recently.³⁶ They are constrained to image domain and their extension to k -space is still an open research challenge.

TABLE 3. Quantitative Measurements at End-Diastole and End-Systole of Septal Wall Thickness, and Right and Left Lumen Diameter Between Septum and the Corresponding Lateral Wall

Case #	End-diastole			End-systole		
	Septal midventricular wall thickness (mm)	Right lumen diameter (mm)	Left lumen diameter (mm)	Septal midventricular wall thickness (mm)	Right lumen diameter (mm)	Left lumen diameter (mm)
1	2.5	10	13	3	8	6
2	2	15	10	3	13	7
3	2.5	16	8.5	3	12	7.5
4	2.5	9.5	10	2.5	9	10
5	2.5	8	13	3	12.5	7.5
6	2.5	11.5	10.5	3	8.5	9
7	2.5	13.5	12	3	10.5	9
8	2.5	16	5.5	3	12.5	5.5
9	2.5	14	10.5	3	12	8
Median (range)	2.5 (2–2.5)	13.5 (8–16)	10.5 (5.5–13)	3 (2.5–3)	12 (8–13)	7.5 (5.5–10)
Free-breathing acquisition	End-diastole			End-systole		
	Septal midventricular wall thickness (mm)	Right lumen diameter (mm)	Left lumen diameter (mm)	Septal midventricular wall thickness (mm)	Right lumen diameter (mm)	Left lumen diameter (mm)
1	3	11	13	3	9	5
2	2.5	15	11	3.5	14	8.5
3	2.5	15	9.5	3	13.5	7
4	2.5	9.5	9.5	2.5	8	10
5	2.5	9.5	13.5	3	11	7.5
6	3	10.5	11	3	7	8.5
7	2.5	14.5	11.5	3.5	11.5	8.5
8	2.5	16	6	3	12.5	6
9	2.5	15	10.5	3	11	9.5
Median (range)	2.5 (2.5–3)	14.5 (9.5–16)	11 (6–13.5)	3 (2.5–3.5)	11 (7–14)	8.5 (5–10)

All *P* > 0.28 between breath-hold and free-breathing acquisitions.

Another promising direction towards images of higher quality is the application of the proposed method on data acquired by 3T MRI scanners. The reported gains in SNR come with increased artifacts (main magnetic and RF field inhomogeneities). These MRI artifacts may influence more fetal MRI, as the FOV tends to be larger than those used in other studies.³⁷ The increased SNR may allow for higher image resolution and acquisition time reduction. However, the existence of stronger eddy currents may require the proper adaptation of the tiny golden angle radial sampling scheme to cope with the resulting artifacts and gradient delays.

This study has a few limitations. First, volunteers were included in this technical development study based on the availability of the MRI scanner during the last few weeks of pregnancy. Early gestation scans were not performed. Second, in several cases, as seen in Table 1, the movement of the fetus was continuous, rendering the analysis of the acquired data impossible. New methods to obviate this type of motion need to be developed in the future. Last, there were cases with extreme fetal movements which also caused DUS signal loss. This could potentially be addressed with a new design of the DUS probe.

In conclusion, a DUS-gated retrospective fetal cardiac MRI reconstruction method was proposed as an improvement to the breath-hold self-gated reconstruction method.¹³ The proposed method was capable of reconstructing free-breathing fetal cardiac cine acquisitions successfully and fetal movement was dealt with either through data rejection or motion estimation and correction. The added convenience of free-breathing data acquisition could help increase fetal cardiac MRI acceptance in the clinic.

Acknowledgment

The authors thank Siemens Healthcare for providing support within the Master Research Agreement with Lund University and the Region of Skåne.

References

1. Wielandner A, Mlczoch E, Prayer D, Berger-Kulemann V. Potential of magnetic resonance for imaging the fetal heart. *Semin Fetal Neonatal Med* 2013;18:286–297.
2. Lloyd DFA, van Amerom JFP, Pushparajah K, et al. An exploration of the potential utility of fetal cardiovascular MRI as an adjunct to fetal echocardiography. *Prenat Diagn* 2016;36:916–925.
3. Hunter LE, Simpson JM. Prenatal screening for structural congenital heart disease. *Nat Rev Cardiol* 2014;11:323.
4. Bhat M, Haris K, Bidhult S, Liuba P, Aletras AH, Hedström E. Fetal iGRASP cine CMR assisting in prenatal diagnosis of complicated cardiac malformation with impact on delivery planning. *Clin Physiol Funct Imaging* 2019;39:231–235.
5. Sharland GK, Allan LD. Normal fetal cardiac measurements derived by cross-sectional echocardiography. *Ultrasound Obstet Gynecol* 1992;2:175–181.
6. Malamateniou C, Malik SJ, Counsell SJ, et al. Motion-compensation techniques in neonatal and fetal MR imaging. *Am J Neuroradiol* 2013;34:1124–1136.
7. Estrin GL, Allsop J, Malamateniou C, Hajnal J, Rutherford M. Assessment of fetal motion to improve the quality of diffusion tensor techniques in fetal MRI. *Arch Dis Child — Fetal Neonatal Ed* 2012;Suppl 1: A16–A17.
8. Yamamura J, Kopp I, Frisch M, et al. Cardiac MRI of the fetal heart using a novel triggering method: Initial results in an animal model. *J Magn Reson Imaging* 2012;35:1071–1076.
9. Reed K, Kochetkova I, Whitby E, et al. Visualising uncertainty: Examining women's views on the role of Magnetic Resonance Imaging (MRI) in late pregnancy. *Social Science and Medicine* 2016;164:19–26.
10. Roy CW, Seed M, van Amerom JFP, et al. Dynamic imaging of the fetal heart using metric optimized gating. *Magn Reson Med* 2013;70:1598–1607.
11. Yang AC, Kretzler M, Sudarski S, Gulani V, Seiberlich N. Sparse reconstruction techniques in magnetic resonance imaging. *Invest Radiol* 2016;51:349.
12. Feng L, Grimm R, Block KT, et al. Golden-angle radial sparse parallel MRI: Combination of compressed sensing, parallel imaging, and golden-angle radial sampling for fast and flexible dynamic volumetric MRI. *Magn Reson Med* 2014;72:707–717.
13. Haris K, Hedström E, Bidhult S, et al. Fetal Cardiac Magnetic Resonance Imaging with self-gated iGRASP. In: *Proc ISMRM 24th Annual Meeting*, Singapore; 2016.
14. Haris K, Hedström E, Bidhult S, et al. Self-gated fetal cardiac MRI with tiny golden angle iGRASP: A feasibility study. *J Magn Reson Imaging* 2017;46:207–217.
15. Otazo R, Kim D, Axel L, Sodickson DK. Combination of compressed sensing and parallel imaging for highly accelerated first-pass cardiac perfusion MRI. *Magn Reson Med* 2010;64:767–776.
16. Otazo, Ricardo SD. Distributed compressed sensing for accelerated MRI. In: *Proc 17th Annual Meeting ISMRM*, Honolulu; 2009. p 378.
17. Winkelmann S, Schaeffter T, Koehler T, Eggers H, Doessel O. An optimal radial profile order based on the golden ratio for time-resolved MRI. *IEEE Trans Med Imaging* 2007;26:68–76.
18. Wundrak S, Paul J, Ulrici J, Hell E, Rasche V. A small surrogate for the golden angle in time-resolved radial MRI based on generalized Fibonacci sequences. *IEEE Trans Med Imaging* 2015;34:1262–1269.
19. Larson AC, White RD, Laub G, McVeigh ER, Li D, Simonetti OP. Self-gated cardiac cine MRI. *Magn Reson Med* 2004;51:93–102.
20. Roy CW, Seed M, Macgowan CK. Accelerated MRI of the fetal heart using compressed sensing and metric optimized gating. *Magn Reson Med* 2016;77:2125–2135.
21. Roy CW, Seed M, Kingdom JC, Macgowan CK. Motion compensated cine CMR of the fetal heart using radial undersampling and compressed sensing. *J Cardiovasc Magn Reson* 2017;19:29.
22. Hansen MS, Sørensen TS, Arai AE, Kellman P. Retrospective reconstruction of high temporal resolution cine images from real-time MRI using iterative motion correction. *Magn Reson Med* 2012;68:741–750.
23. Kording F, Yamamura J, De Sousa MT, et al. Dynamic fetal cardiovascular magnetic resonance imaging using Doppler ultrasound gating. *J Cardiovasc Magn Reson* 2018;20:17.
24. van Amerom JFP, Lloyd DFA, Price AN, et al. Fetal cardiac cine imaging using highly accelerated dynamic MRI with retrospective motion correction and outlier rejection. *Magn Reson Med* 2017;79:327–338.
25. Tsao J, Boesiger P, Pruessmann KP. k-t BLAST and k-t SENSE: Dynamic MRI with high frame rate exploiting spatiotemporal correlations. *Magn Reson Med* 2003;50:1031–1042.
26. Wundrak S, Paul J, Ulrici J, et al. A self-gating method for time-resolved imaging of nonuniform motion. *Magn Reson Med* 2016;76:919–925.

27. Wundrak S, Paul J, Ulrici J, et al. Golden ratio sparse MRI using tiny golden angles. *Magn Reson Med* 2016;75:2372–2378.
28. Huang F, Vijayakumar S, Li Y, Hertel S, Duensing GR. A software channel compression technique for faster reconstruction with many channels. *Magn Reson Imaging* 2008;26:133–141.
29. Kording F, Schoennagel B, Lund G, Ueberle F, Jung C, Adam G. Doppler ultrasound compared with electrocardiogram and pulse oximetry cardiac triggering: A pilot study. *Magn Reson Med* 2015;74:1257–1265.
30. Usman M, Atkinson D, Kolbitsch C, Schaeffter T, Prieto C. Manifold learning based ECG-free free-breathing cardiac CINE MRI. *J Magn Reson Imaging* 2015;41:1521–1527.
31. Fessler J, Sutton B. Nonuniform fast Fourier transforms using min-max interpolation. *IEEE Trans Signal Process* 2003;51:560–574.
32. Lustig M, Donoho D, Pauly JM. Sparse MRI: The application of compressed sensing for rapid MR imaging. *Magn Reson Med* 2007;58:1182–1195.
33. Woodard JP, Carley-Spencer MP. No-reference image quality metrics for structural MRI. *Neuroinformatics* 2006;4:243–262.
34. Crete F, Dolmiere T, Ladret P, Nicolas M. The blur effect: Perception and estimation with a new no-reference perceptual blur metric. *Hum Vis Electron Imaging XII* 2007;6492.
35. Heiberg E, Sjögren J, Ugander M, Carlsson M, Engblom H, Arheden H. Design and validation of segment — Freely available software for cardiovascular image analysis. *BMC Med Imaging* 2010;10:1.
36. van Amerom JFP, Lloyd DFA, Murgasova MK, et al. Fetal whole-heart 3D cine reconstruction using motion-corrected multi-slice dynamic imaging. In: *Proc Jt Annu Meet ISMRM-ESMRMB, Paris, France; 2018; 1052.*
37. Victoria T, Johnson AM, Christopher Edgar J, et al. Comparison between 1.5-T and 3-T MRI for fetal imaging: Is there an advantage to imaging with a higher field strength? *Am J Roentgenol* 2016;206:195–201.